Acoustic Calibration in Shallow Water: Theory, Simulations, and a Preliminary Site Study

by R.P. Porter, D. Rouseff, W.L.J. Fox, and M. Siderius

Technical Memorandum
APL-UW TM31-93
September 1993

Applied Physics Laboratory University of Washington
1013 NE 40th Street Seattle, Washington 98105-6698

Contract N00039-91-C-0072

Acoustic Calibration in Shallow Water: Theory, Simulations, and a Preliminary Site Study

by R.P. Porter, D. Rouseff, W.L.J. Fox, and M. Siderius

Technical Memorandum
APL-UW TM31-93
September 1993

Applied Physics Laboratory University of Washington
1013 NE 40th Street Seattle, Washington 98105-6698

Contract N00039-91-C-0072

ACKNOWLEDGMENTS

This research was sponsored by the Naval Research Laboratory (E.R. Franchi, Code 7105) via the Laboratory's omnibus contract (N00039-91-C-0072) with the Space and Naval Warfare Systems Command.

ABSTRACT

Initial research on a new method for characterizing the acoustic properties of a shallow water site is documented. The method uses moored vertical transmitting and receiving arrays. By combining the array data with limited environmental data, the measured acoustic data are extrapolated to predict the coherent field and transmission loss over an extended region. Motivation for the problem and approach is given, and the theory of the extrapolation algorithm is presented. Numerical examples demonstrate the relative insensitivity of the method to knowledge about the sediment. An experiment to test the extrapolation procedure is contemplated for the summer of 1994, and a possible site off the Massachusetts-New Hampshire coast is considered. Using archival sound speed data and bathymetry, transmission loss is calculated for a region with a gently sloping bottom and is compared with extrapolated predictions. The extrapolation method is shown to be relatively insensitive to sound speed variability in the water column, but sensitive to changes in depth. Element spacing of greater than one-half the acoustic wavelength in both the transmitting and receiving arrays is shown to be adequate for some cases.

CONTENTS

LIST OF FIGURES

LIST OF TABLES

EXECUTIVE SUMMARY

In this document we have considered the problem of calculating the acoustic transmission loss between two points in shallow water. Numerical methods alone are not practical because they require a detailed knowledge of a potentially complicated environment. A new method is developed here that combines limited environmental data with limited acoustic measurements to predict transmission loss over an extended shallow water region. The theory is developed and numerical simulations verify the usefulness of the method.

The theory shows that by using a reference source array and a receiving array, the region of ocean between the two arrays can be "calibrated" for acoustic propagation. In this context, calibration means that a detailed knowledge of the environment is not needed; the effects of the medium on acoustic propagation between the arrays are measured directly. When calculating the transmission loss between points proximate to the two arrays, a large part of the propagation path can be calibrated using this method. The predicted transmission loss is therefore greatly improved. The need for detailed environmental data over the entire propagation path is reduced to needing limited information (depth and sound speed) near the two arrays.

The method is tested by numerical simulation for the case where we have imperfect knowledge of the sediment properties. The simulations show that using conventional methods for predicting the transmission loss can lead to large errors when the detailed sound speed profile of the sediment is unknown. However, when the acoustic calibration method is used, the error is small thereby showing the relative insensitivity of the method to imperfect knowledge of the sediment.

The method is further tested using measured environmental data for the Cape Ann site off the Massachusetts-New Hampshire coast, which is a possible experimental location. As a case study, a region with sloping bottom was selected with the depth increasing from 23 to 112 meters over 23 kilometers in range. The measured sound speed profiles were observed to be strongly range-dependent. Acoustic propagation at 400 Hz was simulated using the parabolic equation method. Transmission loss predictions based on acoustic calibration were in good agreement with exact calculations. Good results were obtained even with sparse sampling (elements spaced every 16 meters) on the receiving array.

1. Introduction

Consider the problem of calculating the acoustic transmission loss between two points in shallow water. Given a complete description of the medium, numerical techniques such as normal modes or the parabolic equation method could be applied. A shallow water site, however, can present an extremely complicated propagation regime. Figure 1.1(a) suggests some of the environmental complexities. Sound will interact with a possibly rough, time-varying sea surface. Reflection from a rough bottom and penetration into an inhomogeneous sediment layer must be considered. Finestructure, internal waves, and solitons will induce sound speed fluctuations in the water column. Consequently, a shallow water site will rarely be known with sufficient detail to make calculations with confidence.

Figure 1.1(b) suggests a possible method for circumventing the lack of environmental data. Transmitting and receiving arrays span the water column. Assume the receiving array can measure the coherent field from any element in the transmitting array. The measurements represent the integrated effects over the indicated range of all the environmental complexities. A detailed knowledge of the medium between the two arrays is therefore not needed since its effects on acoustic propagation are measured directly; the arrays serve to acoustically calibrate the intervening medium [Figure 1.1(c)]. With a rudimentary knowledge of the environment, these data can then be extrapolated to predict the transmission loss between points in the vicinity of the two arrays. The ranges to which the data can be extrapolated will, of course, be a function of medium variability in the regions not probed by the acoustic arrays.

Section 2 gives the basic theory for acoustic calibration. A variationally invariant expression for the extrapolated field is derived. Section 3 contains a series of numerical simulations, with emphasis on the effects of sediment. The available information from the calibration system is shown to significantly improve predictions of transmission loss. Section 4 presents preliminary results from a study of the Cape Ann site, one of several sites under consideration for a field experiment in 1994. Using measured sound speed data, transmission loss calculations are presented and then compared with predictions using the calibration method. Finally, Section 5 briefly summarizes the main results of this study.

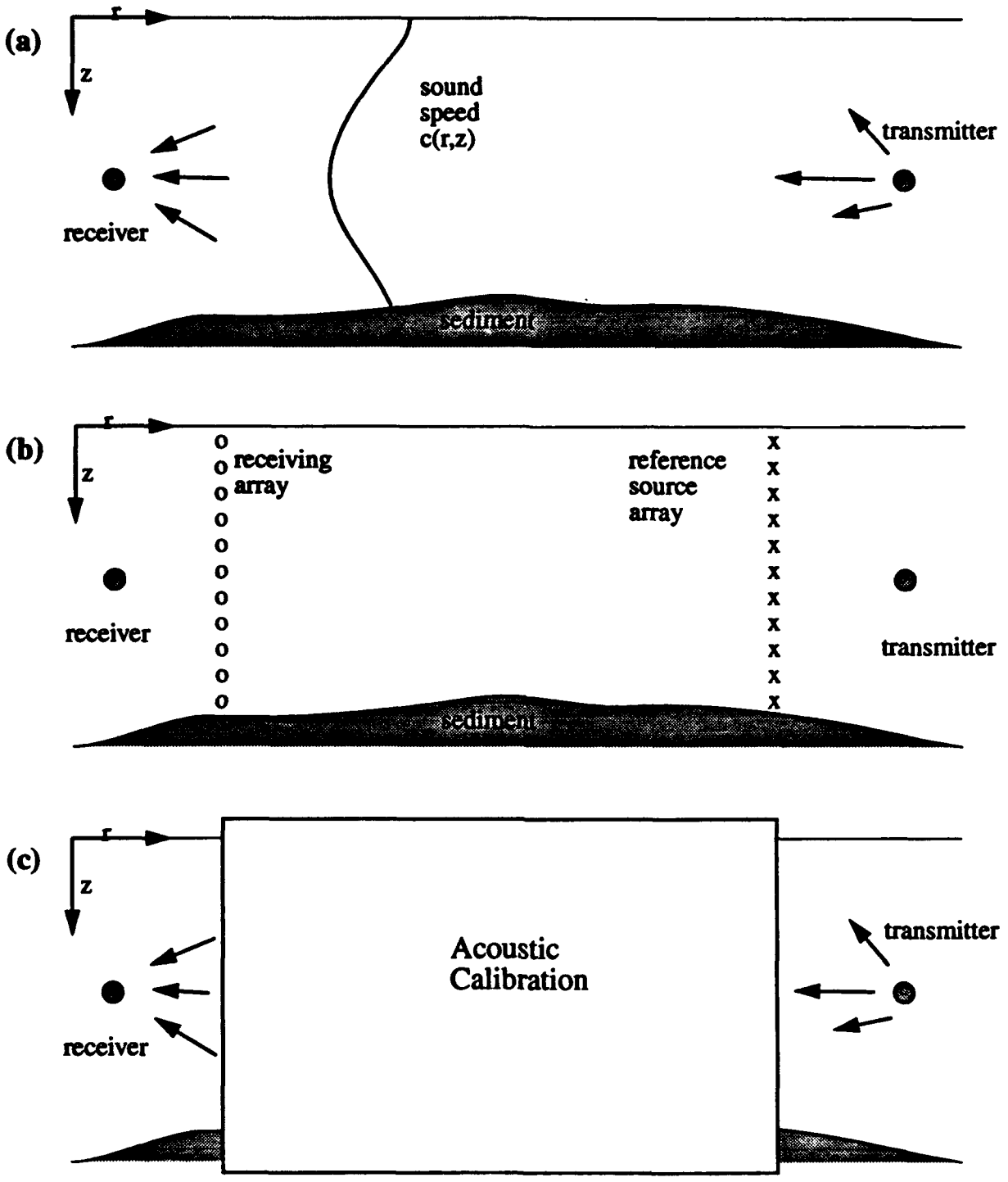

Figure 1.1. (a) Environmental fluctuations complicate propagation calculation. (b) Reference source and receiving array serve to (c) calibrate medium. Variation in medium between reference and receiving arrays effectively removed.

2. Extrapolation Algorithm

Consider the idealized geometry shown in Figure 2.1. A vertical array at range $r = r_1$ transmits a time-harmonic $\exp(-i\omega t)$ signal with a receiving array at $r = 0$. The response from each transmitting element is recorded at each receiving element. The objective is to extrapolate from these measured data to predict what the response along the receiving array would be from a transmitter at the extrapolation point $\mathbf{r}_e = (r_e, z_e)$. A second extrapolation [from the receiving array to a neighboring observation point as shown in Figure 1.1(b)] could be performed, but is omitted here for clarity. Also for simplicity in the derivation, the extrapolation point is taken to lie in the same vertical plane as the two arrays. We assume the arrays span the entire propagation regime and the medium produces no energy loss. Extensions to more practical configurations are discussed later.

The measured response along the receiving array due to the reference is

$$G(z_0;\mathbf{r}_1) = (i2\pi)^{1/2}\sum_m (\xi_m r_1)^{-1/2}\Psi_m(z_0)\,\Psi_m(z_1)\,exp\left(i\int_0^{r_1}\xi_m(r)dr\right), \qquad (2.1)$$

where adiabatic propagation is assumed and the eigenfunctions (modes) Ψ_m and eigenvalues (horizontal wavenumbers) ξ_m are weakly range-dependent. Although the adiabatic approximation is strictly valid only when the medium is rotationally symmetric about the source, it can be used when lateral variability is weak and out-of-plane effects are neglected [Brekovskikh and Lysanov, 1991]. We emphasize that G is a measured quantity; the precise knowledge of the medium that would be required to calculate the individual quantities in the summation has not been assumed. In particular, the eigenvalues depend on the unknown, spatially fluctuating sound speed. Equation

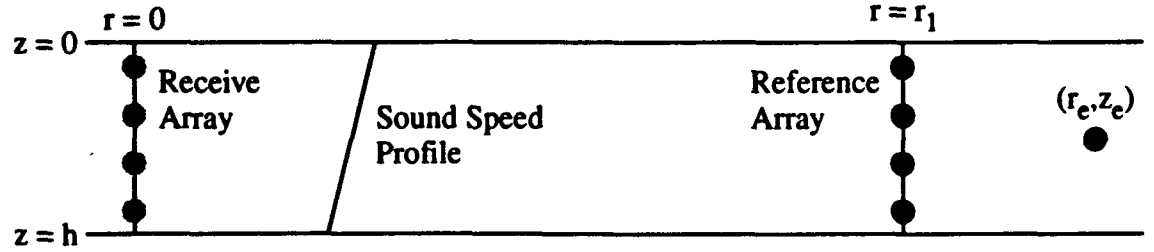

Figure 2.1. Schematic of field extrapolation geometry. Objective is to calculate pressure field due to source at (r_e, z_e) as seen along the receiving array. Response along receiving array from the reference array is measured data which are then used to do the extrapolation calculation.

(2.1) can be interpreted as the measured spatial impulse response or as the Green's function of the inhomogeneous medium.

The first step is to estimate the field that would ensonify the reference array at r_1 from a source at the extrapolation point $\mathbf{r}_e$. The range $r_d = r_e - r_1$ over which the field is extrapolated is typically much less than r_1, the distance between the two arrays. The estimate is generated by introducing the best available environmental information into a propagation routine based, for example, on the parabolic equation or a modal expansion. A modal representation based on a knowledge of the sound speed profile at the reference is

$$\hat{p}_e(\mathbf{r}_1) = (i2\pi)^{1/2} \sum_m (\hat{\xi}_m r_d)^{-1/2} \Psi_m(z_1) \hat{\Psi}_m(z_e) \exp(i\hat{\xi}_m r_d), \tag{2.2}$$

where the caret has been used to denote an estimated quantity. Note that since the only information about the medium is the single sound speed profile, the estimated eigenvalues and eigenfunctions are assumed to be independent of range.

The estimated field at the reference array must be combined with the measured Green's function to produce an estimate of the field at the distant receiving array. One possible algorithm is

$$\hat{p}_e(z_0) = N \int_0^h \hat{p}_e(\mathbf{r}_1) G(z_0; \mathbf{r}_1) \, dz_1, \tag{2.3}$$

where the integration is performed over the length of the reference array, and N is a normalization constant to be defined later. Equation (2.3) can be interpreted as a generalized form of Huygens' principle in optics. The measured data G act like "secondary sources" along the "aperture." These secondary sources effectively sample propagation paths through the inhomogeneous environment between the reference and receiving arrays. The normalization constant is necessary because the standard Huygens formulation requires field data over a plane, while we are using data measured only in depth.

We now show that (2.3) can give a reliable estimate of the field produced by a source at the extrapolation point. Combining (2.1)-(2.3) yields an expression for $\hat{p}_e$ involving an integral over the reference array and a double summation. Using the orthonormality of the eigenfunctions yields

$$\hat{p}_e(z_0) = (i2\pi)^{1/2}\sum_m (\xi_m r_e)^{-1/2}\Psi_m(z_0)\hat{\Psi}_m(z_e)\theta_m \exp\left(i\int_0^{r_1}\xi_m(r)dr + i\hat{\xi}_m r_d\right), \qquad (2.4)$$

with $N = (-ikr_1 r_d/(2\pi r_e))^{1/2}$ for proper normalization, k is the reference wave number and, in analogy with optics, $\theta_m = (k/\xi_m)^{1/2}$ is called the "obliquity factor" [Goodman, 1968]. For lower order modes with predominately horizontal propagation, the obliquity factor is approximately one.

To evaluate the usefulness of (2.4), consider the field produced by a source at the extrapolation point

$$p_e(z_0) = (i2\pi)^{1/2}\sum_m (\xi_m r_e)^{-1/2}\Psi_m(z_0)\Psi_m(z_e)\exp\left(i\int_0^{r_e}\xi_m(r)dr\right). \qquad (2.5)$$

Comparing (2.4) and (2.5) shows the estimated and true fields to have similar modal expansions. The amplitude of each mode in the estimate differs from the true value primarily by the obliquity factor. The accumulated phase of each mode is exactly the same over the common part of the propagation path between the receiver and the reference array. If the medium is relatively quiescent, the estimated phase accumulated between the reference array and the extrapolation point should be in good agreement with the true value.

The only environmental information used to generate the estimate is the sound speed profile at the reference array. By combining these sparse environmental data with the measured response from the reference array, a potentially useful estimate for the field has been derived.

The measured G can be combined with calculated quantities in other ways to produce other estimates of the field. Consider an alternative extrapolation procedure

$$\hat{p}'_e(z_0) = N\int_0^h G(z_0;\mathbf{r}_1)\frac{\partial \hat{p}_e(\mathbf{r}_1)}{\partial r_1}dz_1. \qquad (2.6)$$

Since $\hat{p}_e(\mathbf{r}_1)$ is purely a computed quantity, its derivative can be reliably calculated. Substituting (2.1) and (2.2) into (2.6), neglecting small amplitude terms in the derivative, and again using orthonormality yields the alternative estimate

$$\hat{p}'_e(z_0) = (i2\pi)^{1/2}\sum_m (\xi_m r_e)^{-1/2}\Psi_m(z_0)\Psi_m(z_e)\theta'_m \exp\left(i\int_0^{r_1}\xi_m(r)dr + i\hat{\xi}_m r_d\right), \qquad (2.7)$$

where N' from (2.6) was defined for proper normalization and the new obliquity factor is $\theta'_m = (k/\xi_m)^{-1/2}$. The two estimates, (2.4) and (2.7), differ only in the obliquity factor. As in classical optics theory, alternative formulations result in alternative obliquity factors. The resulting two estimates differ in how they treat higher order modes. Since the eigenvalues are constrained to be less than k and further decreasing with mode number, $\theta_m > 1$ while $\theta'_m < 1$. Hence the estimate in (2.3) puts too great a weight on higher order modes with the converse true for (2.6). Consider then an averaged estimate $\hat{p}_e^V$:

$$\hat{p}_e^V(z_0) = \frac{1}{2}(\hat{p}_e(z_0) + \hat{p}'_e(z_0)), \qquad (2.8)$$

with the resulting obliquity factor θ_m^V,

$$\theta_m^V = \frac{1}{2}(\theta_m + \theta'_m). \qquad (2.9)$$

To consider the averaged estimate in more detail, write the eigenvalues as a perturbation from the free space wavenumber: $\xi_m = k(1-\varepsilon_m)$. Expanding the obliquity factors yields

$$\theta_m = 1 + \frac{1}{2}\varepsilon_m + O(\varepsilon_m^2)$$

$$\theta'_m = 1 - \frac{1}{2}\varepsilon_m + O(\varepsilon_m^2). \qquad (2.10)$$

Substituting into (2.9) shows that first order deviations from unity cancel in the averaged obliquity factor. Consequently the averaged field estimate $\hat{p}_e^V(z_0)$ is invariant to first order errors introduced by the obliquity factors.

Other formulations for the extrapolation algorithm may be appropriate, for example, if the arrays are not perfectly vertical.

3. Numerical Simulations: Effect of Sediment Interaction

This section demonstrates the field extrapolation algorithm in numerical simulations. The emphasis is on evaluating the effect of errors due to sediment, which is a source of error in two ways. First, the transmitting and receiving arrays will not extend into the sediment; hence the arrays are effectively truncated. Thus the orthogonality relationship used to derive the algorithm in Section 2 will not be satisfied exactly. Second, knowledge about the sound speed profile and attenuation in the sediment is often sparse. Imperfect knowledge about the sediment can lead to significant errors in the predicted acoustic field. These difficulties can be partially circumvented using the acoustic calibration scheme detailed in the previous section. This will be demonstrated in the numerical simulations.

Figure 3.1 shows a general idealized geometry for the numerical experiments. The technique consists of a three-step procedure, the first of which is a medium characterization step (or Green's function determination). Each element along the reference array at $r = r_1$ transmits a cw signal of frequency f, and the resulting coherent pressure is recorded at each receiver along the array at $r = 0$. The ocean characterization data are then essentially an MxN matrix of complex values, where M is the number of receivers and N is the number of transmitters. In application, these are measured experimental data. In this study, the data are synthesized numerically. The normal mode program KRAKEN [Porter, 1990] will be used to simulate all propagating acoustic fields in this section.

The second step in the extrapolation technique is to estimate the field at the transmitter locations

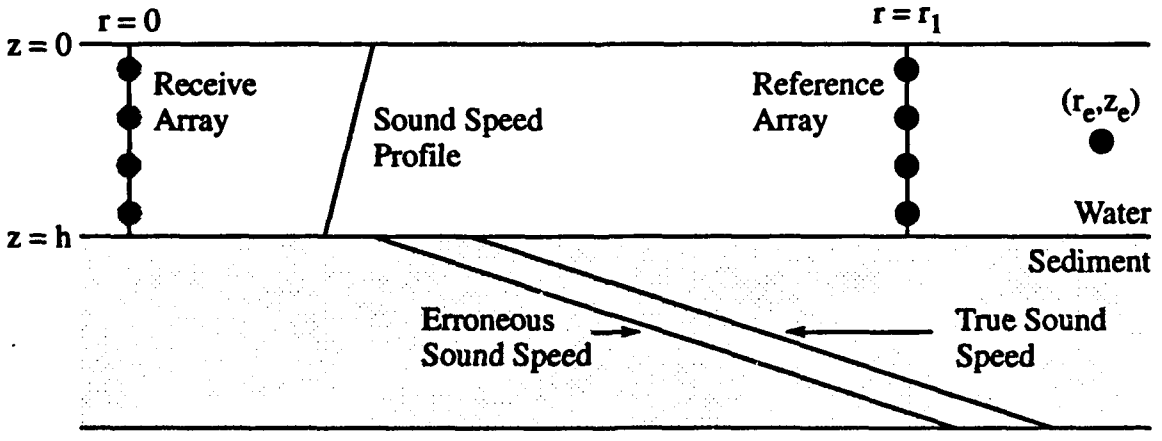

Figure 3.1. General idealized geometry for numerical simulations.

on the reference array that would be produced by a source at the extrapolation point, (r_e, z_e). This is a simulation step even in actual applications. Estimates of the water and sediment properties in the vicinity of the reference array are assumed to be range independent over the distance $r_d = r_e - r_1$ and are used as inputs to the propagation code. An "erroneous sound speed" as in Figure 3.1 will be used for this step in the present simulations to show the extrapolation technique's relative insensitivity to errors in environmental parameters as compared to conventional techniques of acoustic field prediction.

The third and final step in the extrapolation procedure is integration in depth of the product of the pressure (or normal gradient of the pressure) and the Green's function as shown in Equations (2.3) and (2.6). Since this product is known at a discrete set of depths, the integral must be approximated by numerical quadrature. The extrapolation results to be shown in this section are computed using the averaged estimate of Equation (2.8).

Table 3.1 shows the experimental parameters in the water for the two scenarios exhibited here. Scenario 1 has a 300 m deep water column and is typical of depths near the prospective Point Loma site. Scenario 2 has water 30 m deep. Since the emphasis in this section is on the effects from the sediment, both scenarios have range-independent sound speed profiles in the water. Furthermore, it is assumed "perfect knowledge" about the sound speed is available. By making this assumption, the effects of the sediment can be isolated. Range-dependent sound speed profiles are considered in Section 4. The entries for $c(0)$ and $c(h)$ are the endpoints of the sound speeds in the water, which are then linear in between. Note that the sound speeds are downward refracting, forcing the transmitted sound to interact with the sediment.

Table 3.1. Environmental parameters for simulations

	f (Hz)	h (m)	r_1 (km)	r_e (km)	z_e (m)	$c(0)$ (m/s)	$c(h)$ (m/s)
Scenario 1	300	300	20	25	150	1500	1480
Scenario 2	400	30	10	12.5	15	1500	1490

Table 3.2 shows the parameters for the simulated sediment layer. These parameters are the same for both simulation scenarios. As suggested in Figure 3.1, the "true" sound speed increases linearly with depth in the sediment. The sound speed at the interface is 1540 m/s. The "measured" data from the reference array will be affected by this true sound speed profile. To test the effect of imperfect knowledge of the sediment, the assumed sound speed in the sediment is in error. The erroneous sound speed has the correct gradient but is offset by 10 m/s at the interface.

Table 3.2. Sediment properties for simulations

"True" $c(h)$	Erroneous $c(h)$	Δc (z) ((m/s)/m)	Atten. (dB/λ)	Density (g/cm^3)
1540	1530	1.6	0.1	1.5

Figure 3.2 shows the simulation results for scenario 1, which are comparisons of transmission loss vs depth along the receive array at $r = 0$ due to a source at $r_e = 25$ km and depth $z_e = 150$ m. The black lines are transmission loss calculated using KRAKEN with perfect knowledge of the medium (i.e., the "true" sediment sound speed is used in the calculation), and is taken as ground truth. The gray lines show an estimate of the transmission loss using the erroneous estimate of the sediment sound speed. Figure 3.2(a) shows the performance of a conventional method for predicting transmission loss, i.e., using estimated environmental parameters as input to a propagation code, in this case KRAKEN. As can be seen in this plot, a relatively small error in the discontinuity in the sound speed at the interface can result in significant departure from the true transmission loss curve. A small error in knowledge about the medium can have a significant

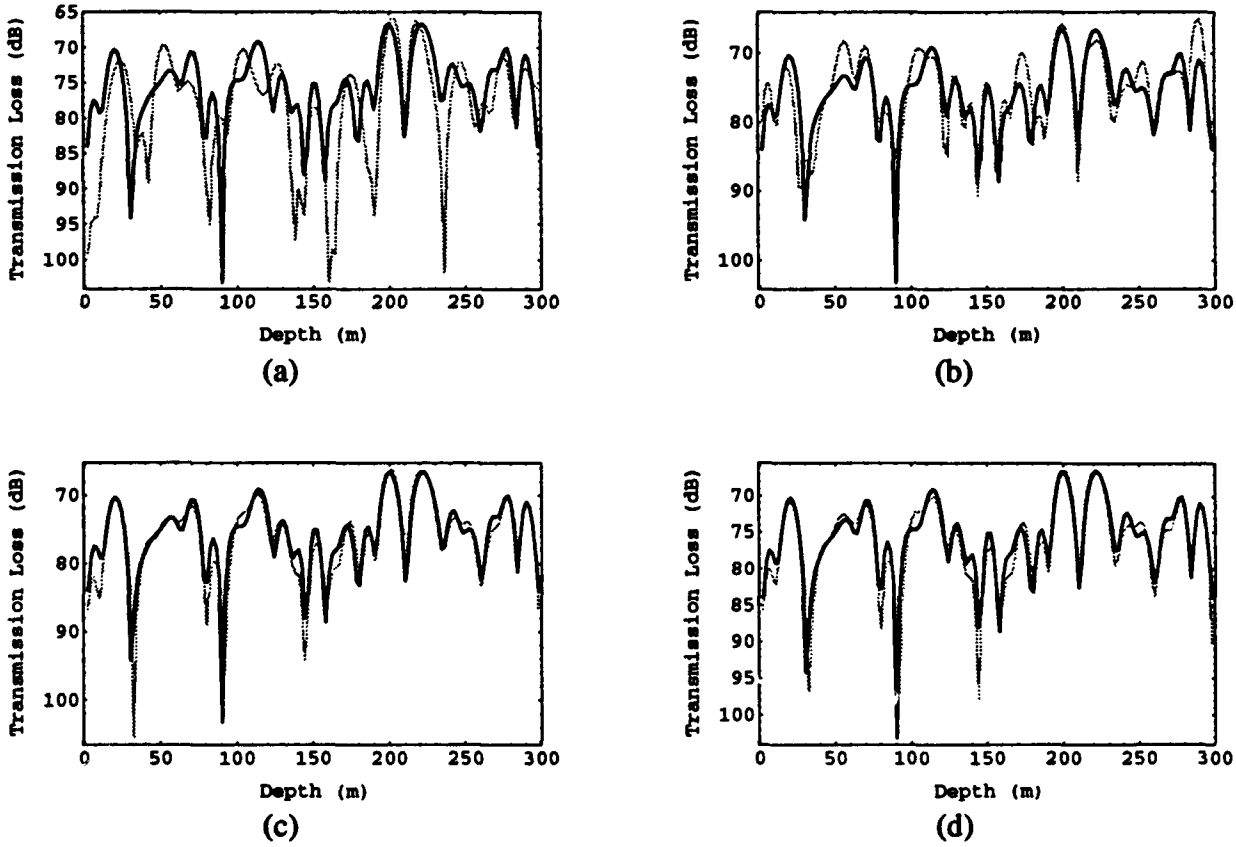

Figure 3.2. Simulation results for scenario 1: (a) no calibration, (b) calibration with 2λ reference array, (c) calibration with λ reference array, (d) calibration with $\lambda/2$ reference array.

cumulative effect when taken over a significant range, here 25 km.

Figures 3.2(b), (c), and (d) demonstrate the extrapolation technique of transmission loss prediction. The examples use progressively more dense sampling on the reference array: (b) uses 10 m ($\sim 2\lambda$) spacing, (c) uses 5 m ($\sim\lambda$) spacing, and (d) uses 2.5 m ($\sim\lambda/2$) spacing. The reference array is 20 km from the receiver, and the ocean characterization step effectively "calibrates" this part of the medium. Consequently, the erroneous sound speed information is used only over the 5 km between the reference array and the extrapolation point. It appears that for this scenario the increase in reference array sampling from λ spacing to $\lambda/2$ spacing does not have an appreciable effect.

Figure 3.3 shows results of experiments similar to Figure 3.2 using the environmental parameters for scenario 2 (see Table 3.1). The appearance of the transmission loss vs depth curves is much smoother due to the fact that many fewer modes propagate in 30 m of water. The spacings of transmitters on the reference array for this scenario are as follows: (b) uses 4 m ($\sim\lambda$) spacing, and (c) uses 2 m ($\sim\lambda/2$) spacing. As for the previous case, the medium calibration provides for more accurate predictions of the transmission loss.

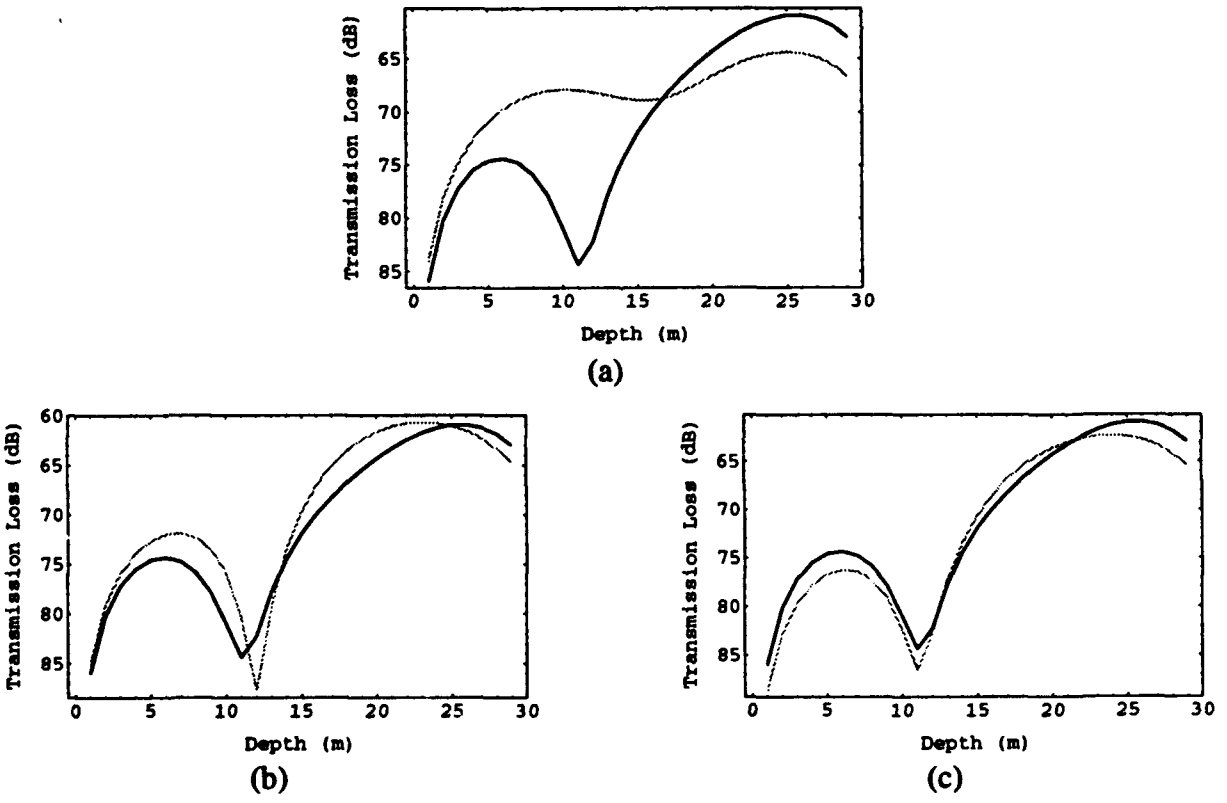

Figure 3.3. Simulation results for scenario 2: (a) no calibration, (b) calibration with λ reference array, (c) calibration with $\lambda/2$ reference array.

4. Preliminary Results from the Study of Cape Ann Site

4.1 Environmental Measurements from Woods Hole Oceanographic Institution

There are several potential sites for an acoustic calibration experiment. In this section, we consider the site between Cape Ann and the mouth of the Merrimack river, near the Massachusetts-New Hampshire border. We selected this site for study primarily because of the available environmental data. This preliminary study should not be interpreted as an endorsement of a particular site; rather it is a first step and a test of our ability to include environmental data in the acoustic simulations.

An extensive series of CTD casts and depth soundings were made at the site in late April 1993 by Dr. W. Rockwell Geyer and the Woods Hole Oceanographic Institution. Figure 4.1 shows the coastline with the region of the cast locations highlighted. Figure 4.2 shows the detailed position of each of the 80 CTD casts. The casts were generally made along a set of trajectories normal to the shoreline.

From the 80 CTD casts, the environmental data from casts 54 to 58 were chosen for use in numerical modeling. The bathymetric and sound speed variations between casts 54 and 58 are well suited for observing the performance of the acoustic calibration method.

These five casts start near the shoreline with cast 58 and proceed out approximately 24 km to cast 54. Along this path, the water depth increases smoothly. The location of the casts and bathymetric data are given in Table 4.1. The location of these casts is contained in NOAA chart 13278. From this chart the ocean depths in between the casts were estimated, and it was found that there are no abrupt bathymetry variations between data points. A plot of the bathymetry as a function of range is given in Figure 4.3.

Data from the casts provided the salinity and temperature of the water at known locations and depths. From this information the sound speed is calculated by

$$\begin{aligned} c(z, T, S) &= 1449.2 + 4.6T - 0.055T^2 + 0.00029T^3 + \\ &\quad (1.34 - 0.010T)(S - 35) + 0.016z, \end{aligned} \tag{4.1}$$

where T is the temperature (degrees Celsius), S is the salinity (parts per thousand), and z is the depth (meters).

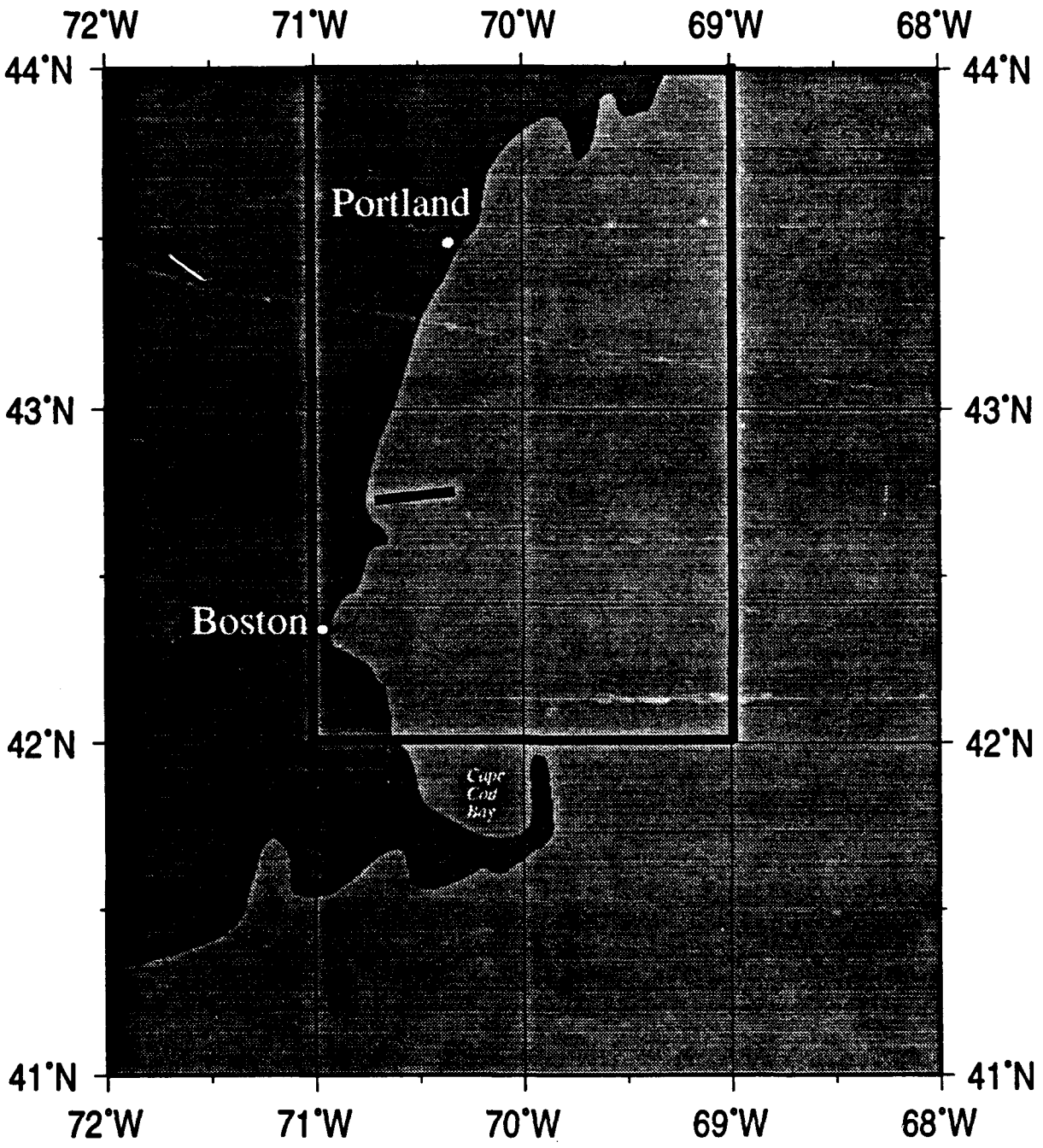

Figure 4.1. Map of the experimental location. The boxed area corresponds to Figure 4.2. The black line is the approximate location of casts 58 to 52.

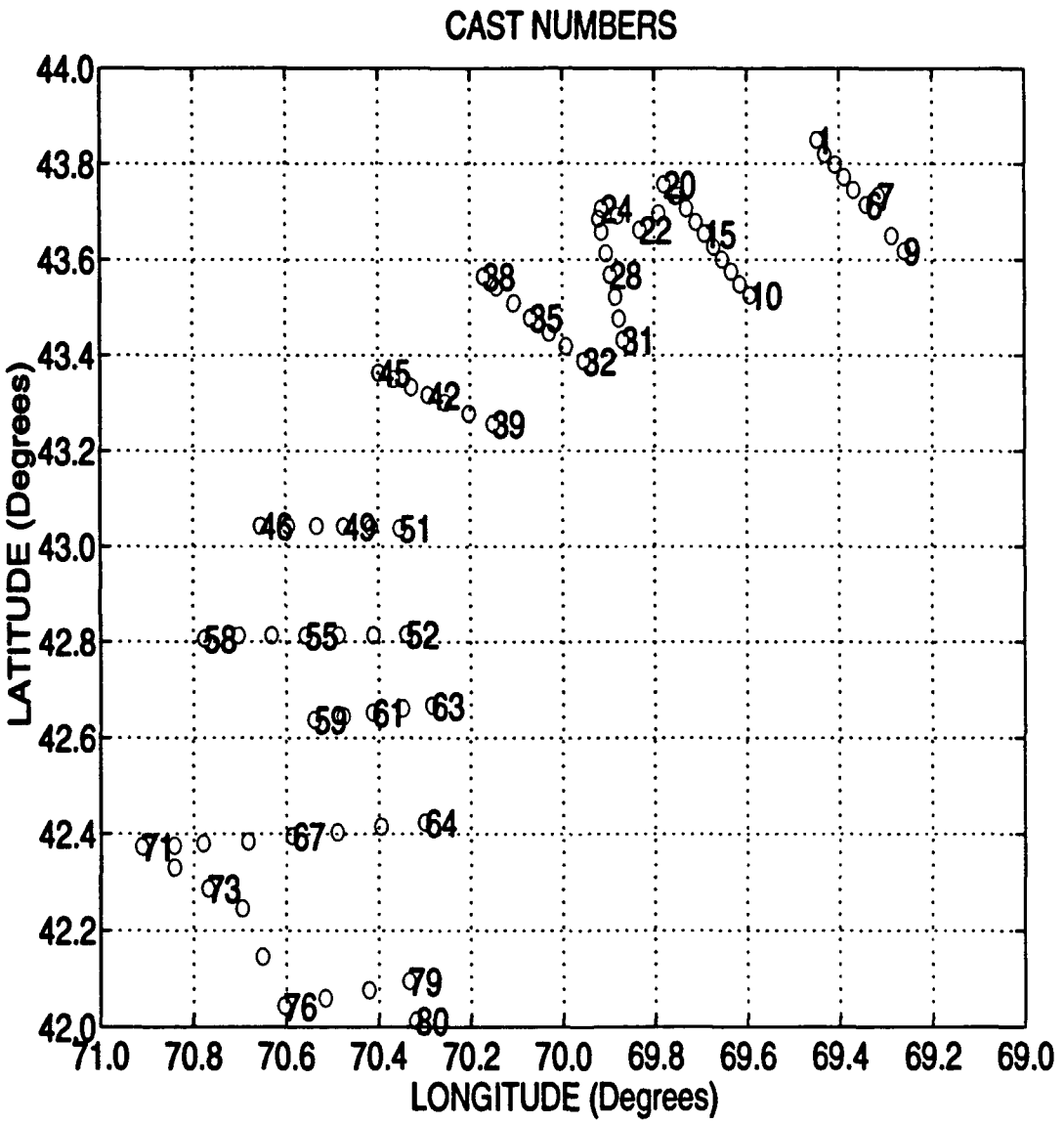

Figure 4.2. Location of cast sites. The shoreline is towards the left side.

Table 4.1. Depth and range data

CTD cast number	latitude (degrees, minutes)	longitude (degrees, minutes)	depth (meters)	range from previous cast (km)	distance from cast 58 (km)
58	42°, 48.402'	70°, 46.602'	23	----	----
57	42°, 48.798'	70°, 42.198'	42	5.859	5.859
56	42°, 48.798'	70°, 37.902'	81	6.003	11.862
55	42°, 48.798'	70°, 33.498'	109	5.857	17.719
54	42°, 48.900'	70°, 29.202'	112	6.048	23.767

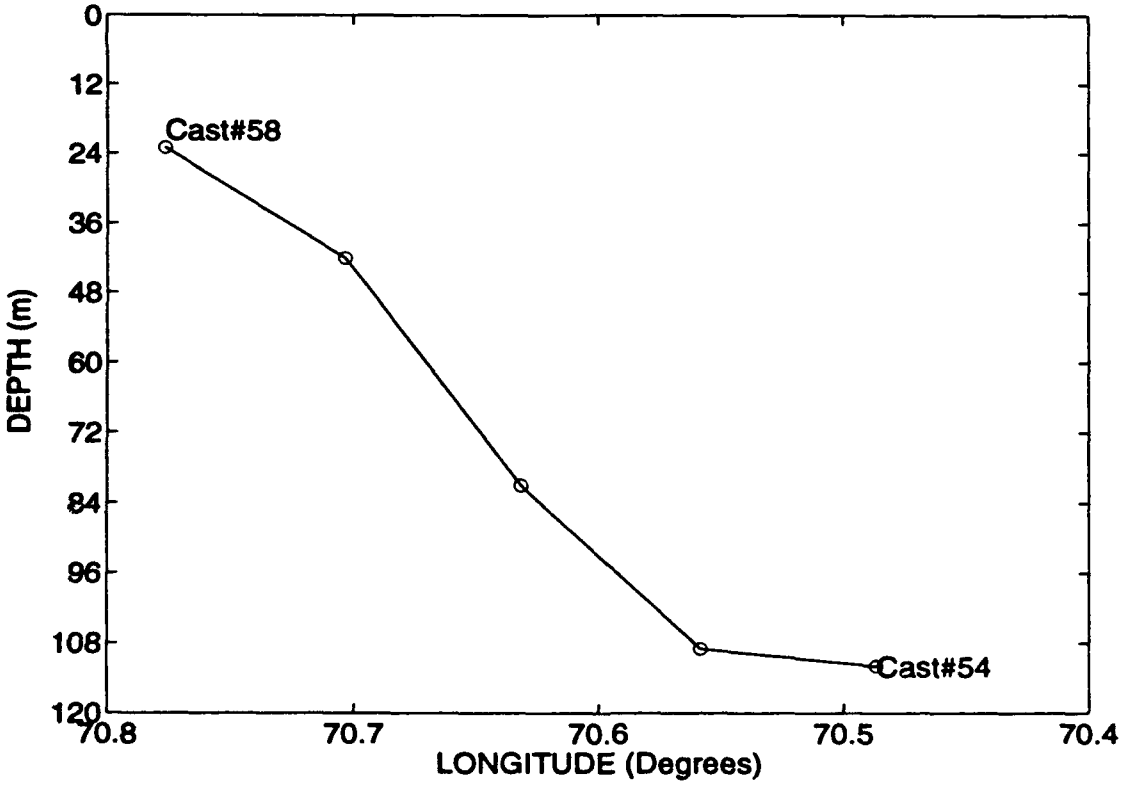

Figure 4.3. Bathymetry points from cast 58 to cast 54.

The sound speed profiles are shown in Figure 4.4. The top plot in Figure 4.4 shows qualitatively how the profiles vary with range and depth. The bottom five plots show the profiles as functions of depth with each plot scaled appropriately. There are several observations that can be made from the sound speed plots. First, the profiles are seen to be range-dependent. Second, they are generally decreasing with depth. Third, there are acoustic channels present, as clearly seen from the profile of cast 57. There is probably a region of relatively large temperature variation in the vicinity of cast 57 causing the sound speed to increase. These channels can trap and propagate acoustic energy, as well as cause coupling of modes.

The measured data show that this site has range-dependent bathymetry and complicated sound speed profiles. In the following subsection, we simulate acoustic propagation at this site using the parabolic equation method.

4.2 Model of the Cape Ann Site

The bathymetry and sound speed profiles are used to model the acoustic wave propagation at the possible experimental site near Cape Ann. The information at the five cast locations is used to create a realistic range dependent model. The FORTRAN program EFEPE [Collins, 1988], which uses the parabolic equation method (PE), is used to find the propagation loss. The sediment density, attenuation, and sound speed are estimated [Dosso and Chapman, 1987]. Since the sediment effects were considered in Section 3, the present simulation isolates the effects of range dependence in the water column. Better information on the sediment is available in a classified data base, and will be used for final studies. Figure 4.5 shows some of the model parameters. The source is at the location of cast 58 at a depth of 10 m, and the vertical receiving array is at the location of cast 54 (Table 4.1).

The transmission loss for this site is displayed in Figure 4.6. The bathymetry and sound speed profiles are interpolated between data points in order to have a smooth range-dependent model. The range and depth are the same as in Figure 4.5.

From the transmission loss plot, it can be seen that the energy is mostly contained in the water column. There is very little penetration into the sediment at ranges of only a few kilometers from the source. Also, the higher order modes penetrate deeper into the sediment and therefore have more attenuation. There is significant energy only in the first five modes at a range of 24 km from the source even though many more are excited at the location of the source. The decrease in maxima and minima of the transmission loss with increasing range is an indication of the mode stripping.

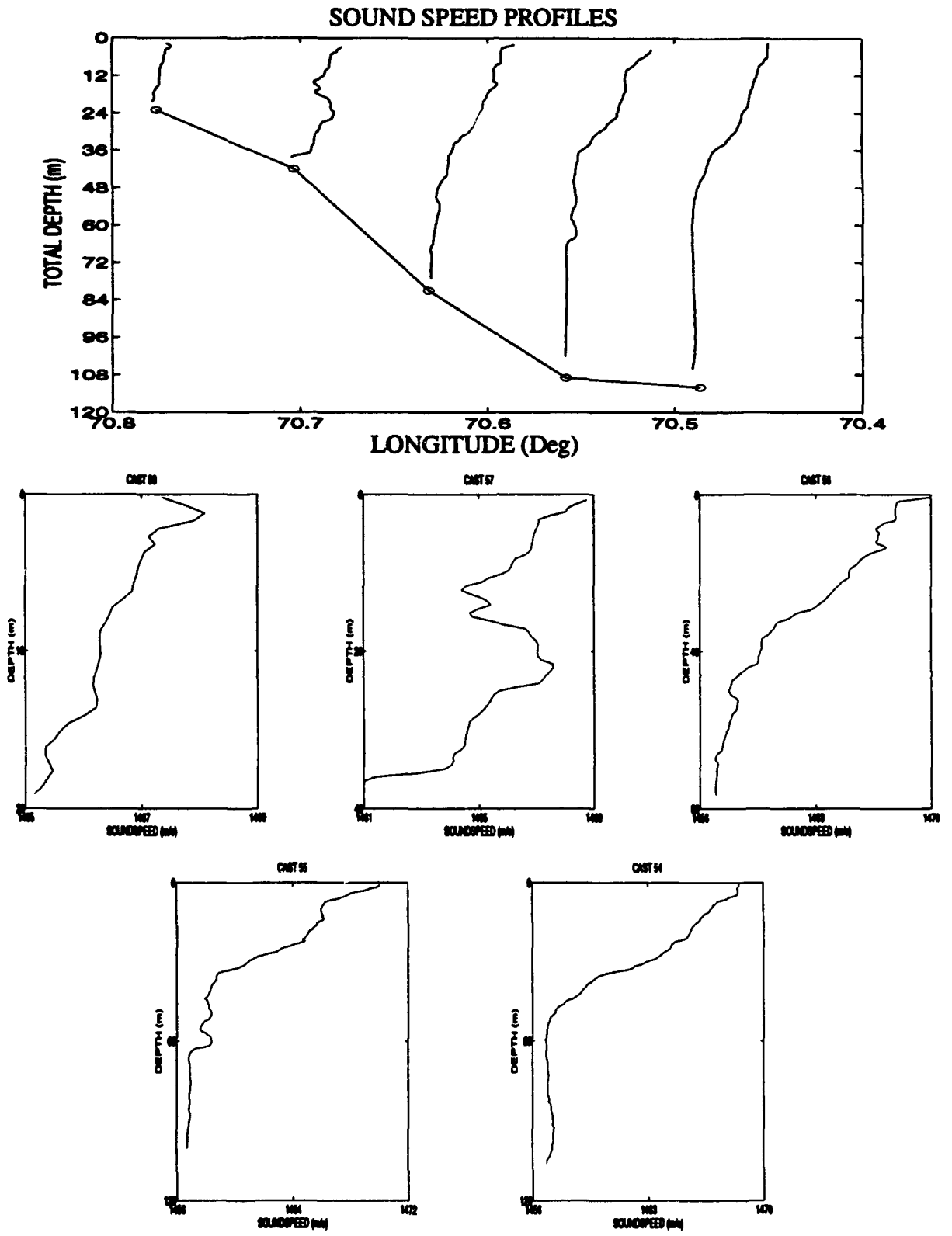

Figure 4.4. Plots of the sound speed profiles with bathymetry (in the top plot all SSPs are scaled the same; in the lower five plots, the depth and sound speed scales are different).

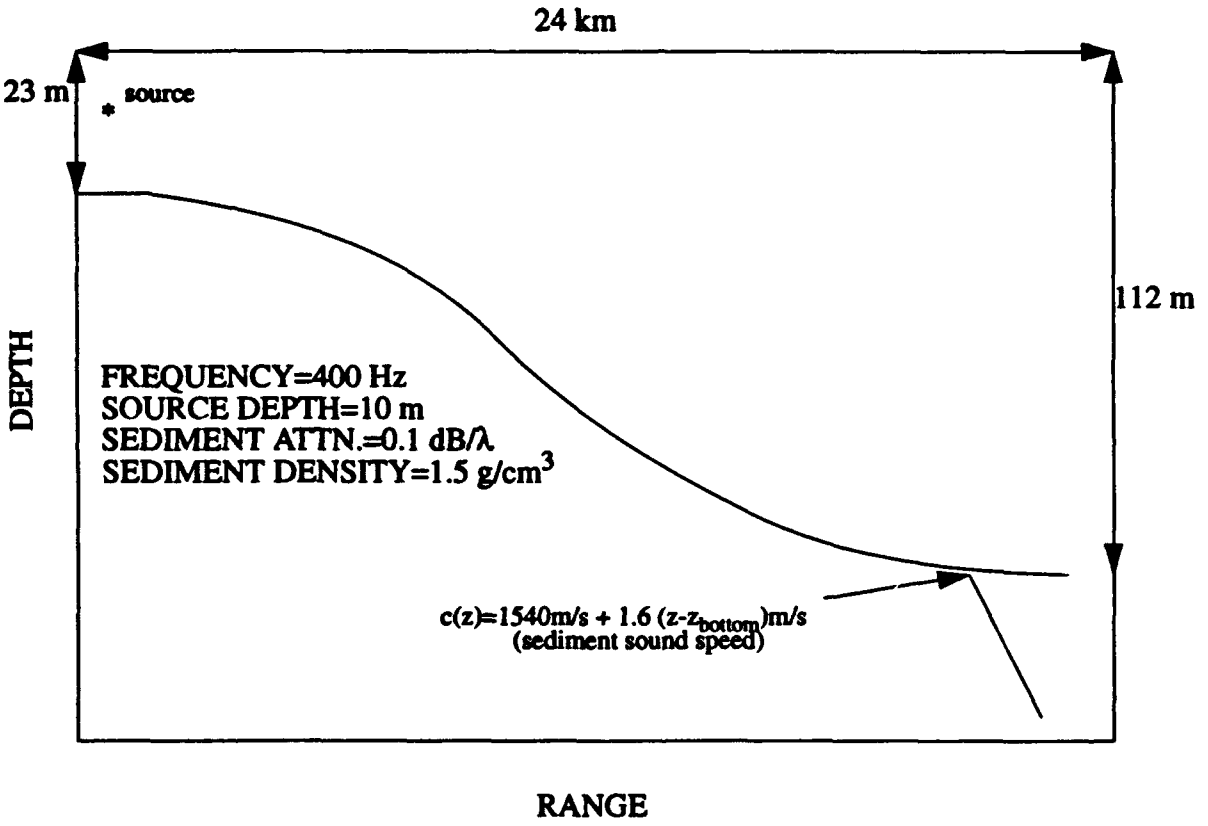

Figure 4.5. Model parameters.

The transmission loss plot also illustrates how the energy seems to follow the curvature of the downward slope. This result is similar to a monotonically increasing depth/linearly decreasing sound speed profile case studied by Brekhovskikh and Lysanov [1991, p. 153, Figure 7.1] using a ray trace.

The results of this section demonstrate our ability to couple environmental measurements to acoustic simulation codes. Our ongoing work is to test the field extrapolation algorithm in such regimes.

4.3 Extrapolation Method for the Cape Ann Site

As noted in the introduction, the field extrapolation method can predict the transmission loss between points in the vicinity of the vertical transmitting and receiving arrays. The data are essentially extrapolated twice: once near the transmitting array, and once near the receiving array. Section 2 developed the basic theory for the subproblem of predicting the response along the receiving array due to a distant source; for this case the data must be extrapolated only in the vicinity of the transmitting array. The simulations in Section 3 considered the same case. In this section, we consider the dual problem. The response from a source is measured along a vertical receiving array. These data are then extrapolated in the vicinity of the receiving array to predict what would be measured if a receiver were placed at the neighboring point. This latter configuration is the most likely one to be tested in the initial field experiments. Suspending an additional hydrophone to test the algorithm is relatively simple compared to bringing in an additional source.

Variability in the sediment and the water column determines the ranges over which the field can be extrapolated. For a location like the Cape Ann site with a sloping bottom, bathymetry is an additional factor. As formulated in Section 2, the extrapolation algorithm does not compensate for changes in depth between the receiving array and the extrapolation point (the uncalibrated region). In this section, we consider two examples. First, the depth of the water is artificially set to be constant beyond the receiving array. This test then isolates the effects of variability in the water column on the extrapolation procedure. In the second case, the actual bathymetry is used. Here the depth of the water increases between the receiving array and the extrapolation point.

The configuration for the first case is shown in Figure 4.7. The extrapolation point at $r=r_2$ is

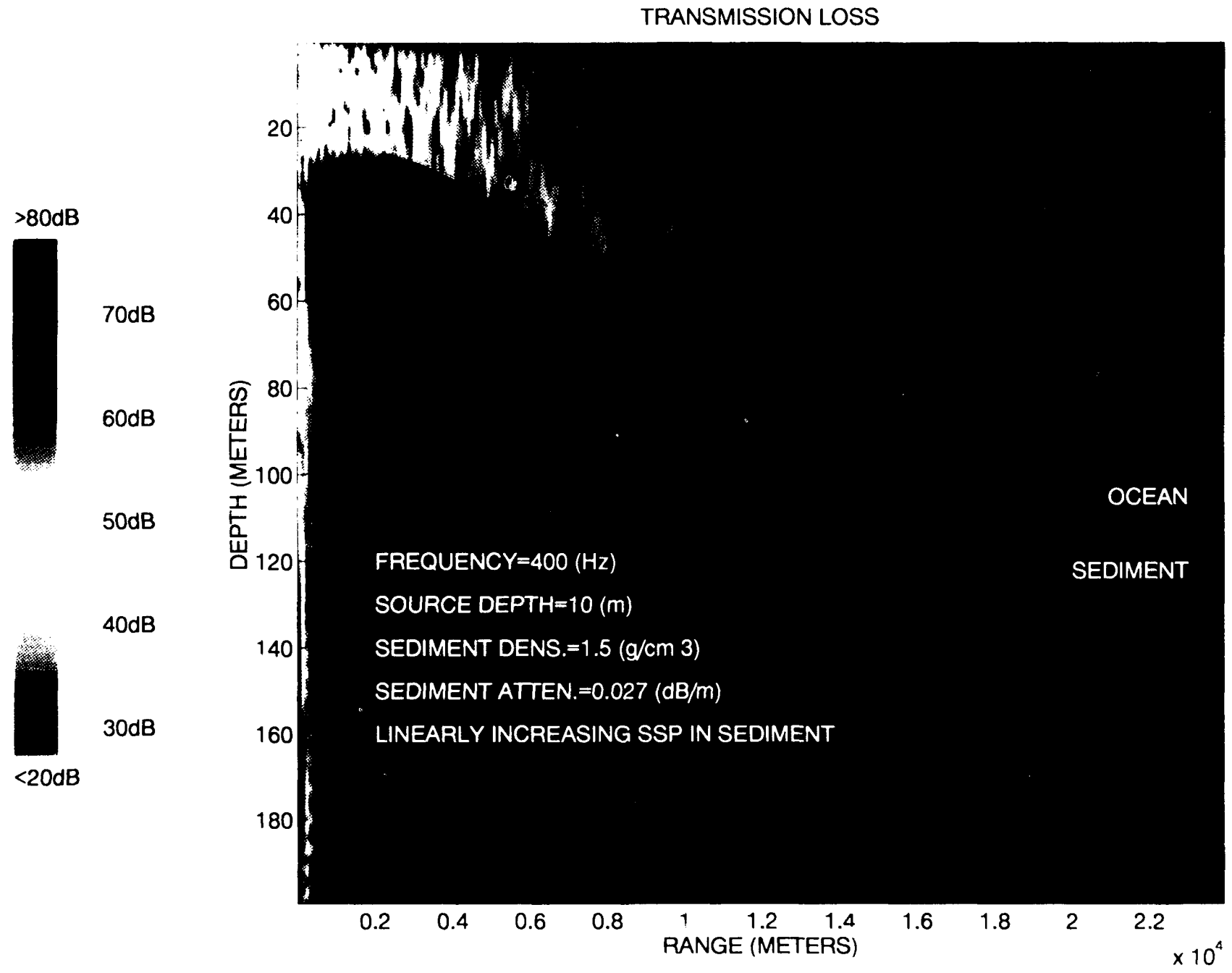

Figure 4.6. Transmission loss for the Cape Ann site. The red line shows the bathymetry.

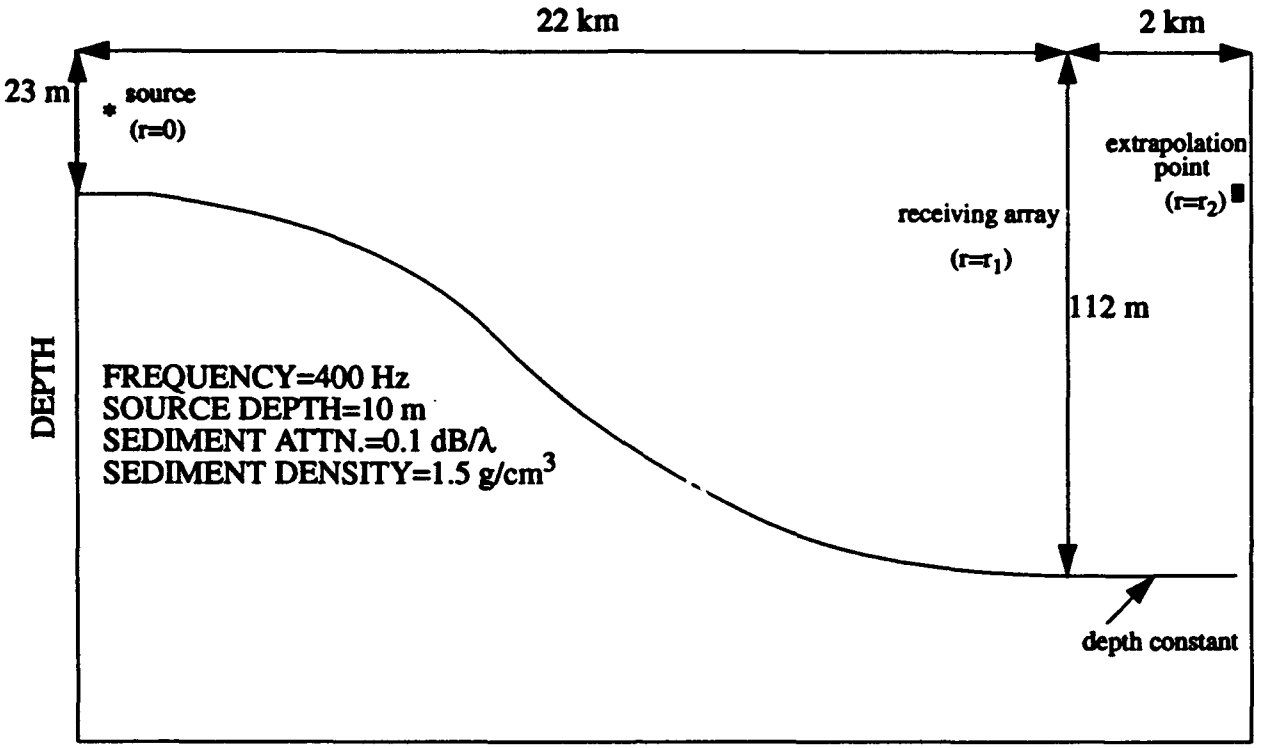

Figure 4.7. Model parameters for extrapolation test. The depth is artificially held constant between receiving array and extrapolation point.

24 km from the source and 2 km from the receiving array. The sound speed profile between the array and the extrapolation point is allowed to vary according to the measured data, but the depth is artificially set to a constant 112 m (the actual depth varies by about 1 m). The PE code is used both to calculate the "ground truth" field at the extrapolation point and to generate the "measured" data along the receiving array. The measured data are then extrapolated to $r=r_2$ and compared with the ground truth. To ensure that the extrapolation method is not dependent on any particular numerical method, the extrapolation was performed using KRAKEN.

The initial test assumed 4 m element spacing along the receiving array. The resulting extrapolated and true fields are shown as a function of depth in Figure 4.8. The results are generally in excellent agreement. The test was repeated using 16 m spacing along the receiving array, with the results shown in Figure 4.9. Since the attenuation in the sediment tends to strip off most of the high order modes, only the low order modes are present at the receiving array. Therefore, the

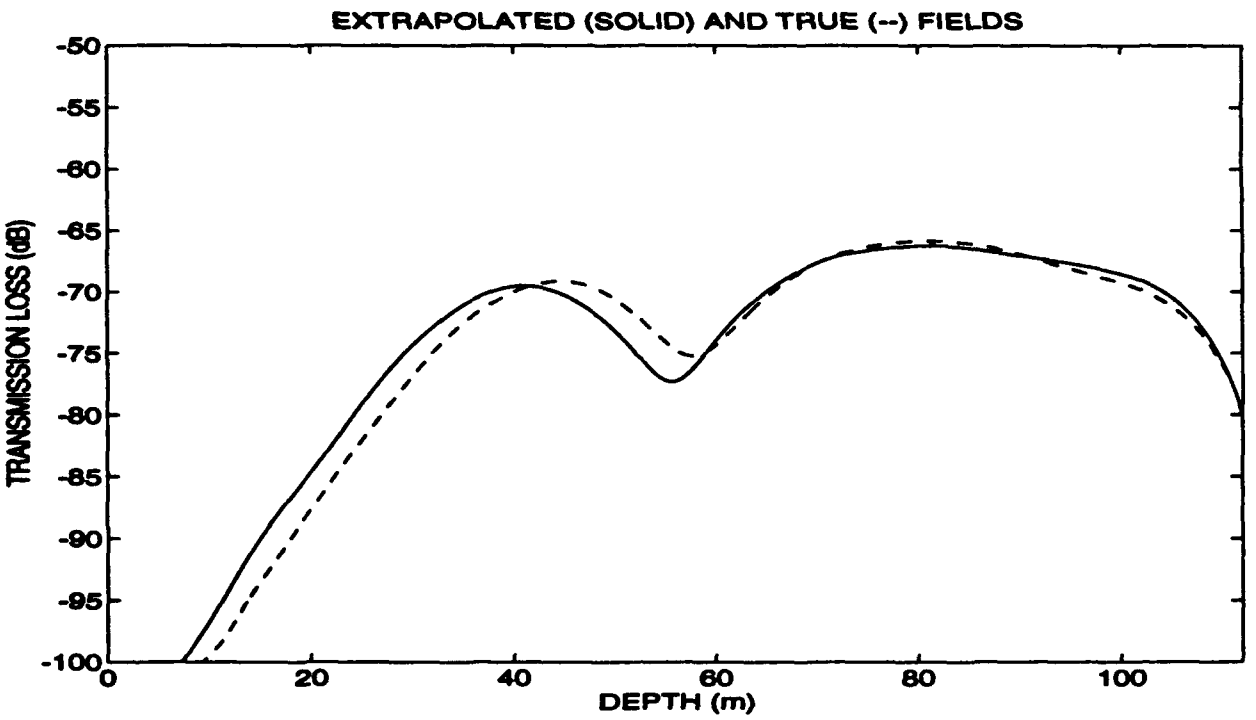

Figure 4.8. True and extrapolated transmission loss curves for 4 m sampling.

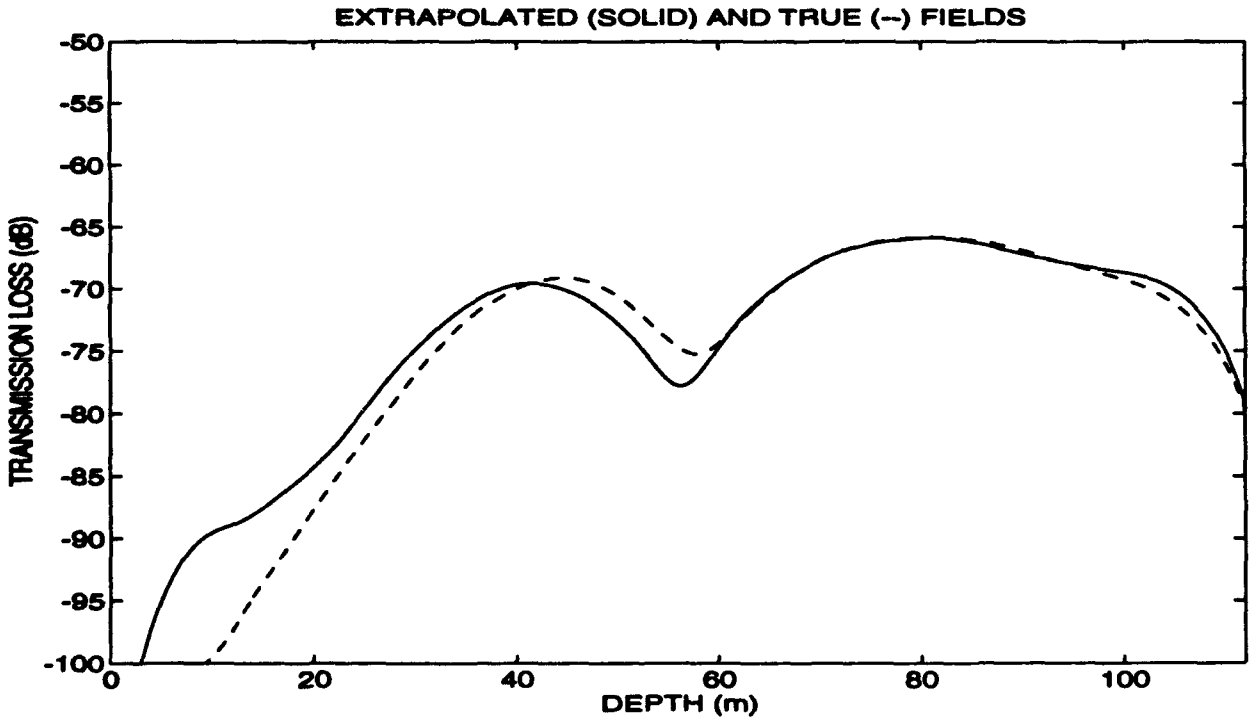

Figure 4.9. True and extrapolated transmission loss curves for 16 m sampling.

array only needs enough receivers to adequately sample the low order modes. The results are reasonable for the 16 m spacing, indicating that at 22 km only the first five or six modes exist.

In the second case, the water depth was allowed to increase. The geometry is shown in Figure 4.10. The distance between the source and the receiving array is 10 km with the extrapolation point an additional 1 km in range. Over this 1 km, the depth of the water column increases from 67 to 74 m. The true and extrapolated fields were computed as before. Note that the extrapolation algorithm as presently formulated assumes no knowledge about the bathymetry. Hence the extrapolated field is calculated assuming (incorrectly) that the depth remains at 67 m. The true and extrapolated fields are shown as functions of depth in Figure 4.11. The agreement is only marginal. Note that the prominent local minimum at 26 m in the true field is shifted by approximately 7 m in the extrapolation. This is the difference between the true depth and what was assumed for the extrapolation.

The last example shows the important role played by the bathymetry in field extrapolation. The results are consistent with the transmission loss plot shown in Figure 4.6; for a downwardly refracting profile and downwardly sloping bottom, the acoustic energy "hugs" the bottom. Hence a lack of knowledge about the depth, even over the limited extrapolation range, can lead to errors in the prediction. These results show that the extrapolation algorithm should be extended to incorporate some knowledge about the bathymetry.

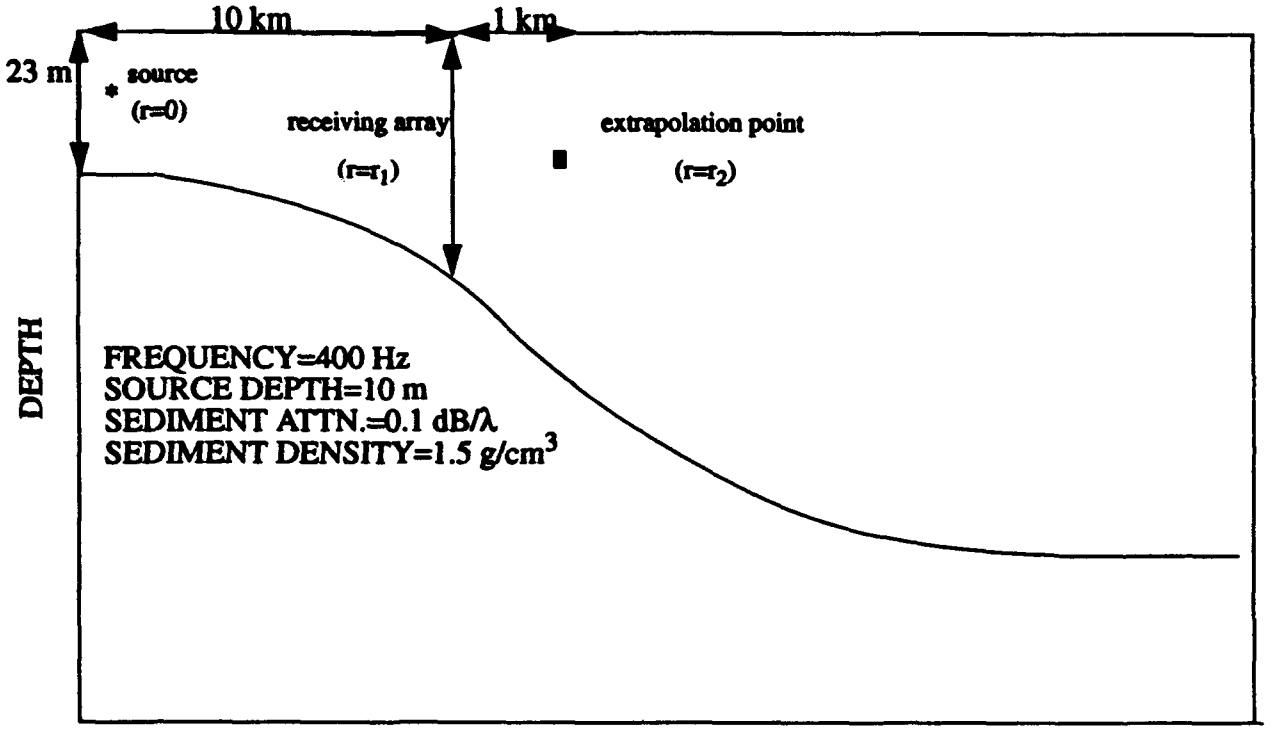

Figure 4.10. Model parameters for extrapolation method.

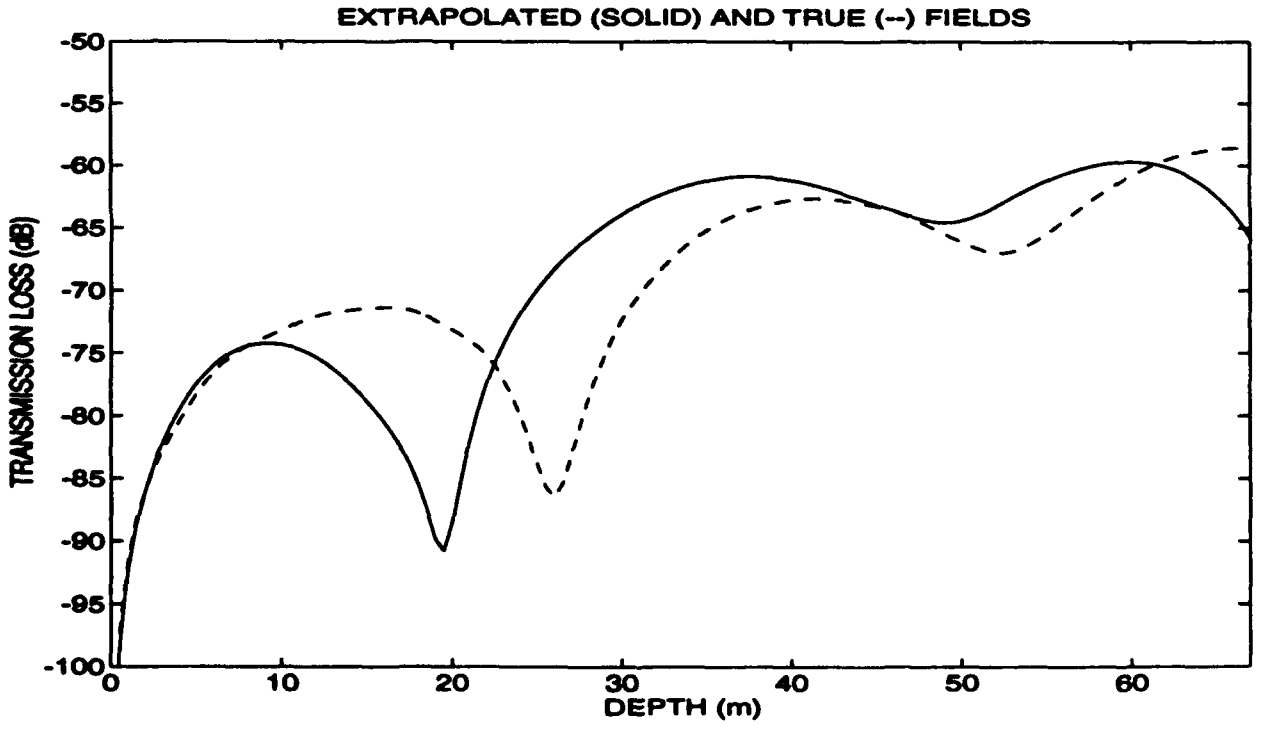

Figure 4.11. True and extrapolated transmission loss curves.

5. Conclusions

• The theoretical basis of the field extrapolation method for characterizing the acoustic properties of a medium has been derived.

• Capability exists to integrate measured sound speed profiles, sediment data sets, and bathymetry information into the acoustic simulations.

• Simulations to date suggest that field extrapolation is relatively insensitive to imperfect knowledge about the sediment.

• Simulations to date suggest that field extrapolation is relatively insensitive to variability in the sound speed profile.

• Transmitting and receiving arrays with coarse sampling (element spacing greater than one-half the acoustic wavelength) may be adequate. Required sampling rate for given location can be estimated from numerical simulations.

• Extrapolation procedure is sensitive to changes in the water depth. Present algorithm assumes depth is constant over extrapolation regime. It should be possible to extend theory by including any a priori knowledge about bathymetry. This is a subject of current research.

References

Brekhovskikh, L. M. and Y. P. Lysanov, "Fundamentals of Ocean Acoustics," Springer-Verlag, New York, 1991.

Collins, M. D., "FEPE User's Guide," NORDA Technical Note 365, Naval Research Laboratory, Stennis Space Center, Mississippi, October, 1988. (For the FEPE computer code, the author may be contacted by e-mail: COLLINS@v5160.nrl.navy.mil)

Dosso, S. E. and N. R. Chapman, "Measurement and modeling of downslope acoustic propagation loss over a continental slope," J. Acoust. Soc. Am., vol. 81, no. 2, 258-268, 1987.

Goodman, J. W., "Introduction to Fourier Optics," McGraw-Hill, New York, 1968.

Porter, M. B., "The KRAKEN Normal Mode Program," Unpublished technical report, SACLANT Undersea Research Centre, 11 Nov. 1992.

REPORT DOCUMENTATION PAGE

Form Approved
OPM No. 0704-0188

1. AGENCY USE ONLY *(Leave blank)*	2. REPORT DATE	3. REPORT TYPE AND DATES COVERED
	September 1993	Technical

4. TITLE AND SUBTITLE
Acoustic Calibration in Shallow Water:
Theory, Simulations, and a Preliminary Site Study

5. FUNDING NUMBERS
SPAWAR
Contract N00039-91-C-0072

6. AUTHOR(S)
R.P. Porter, D. Rouseff, W.L.J. Fox, and M. Siderius

7. PERFORMING ORGANIZATION NAME(S) AND ADDRESS(ES)
Applied Physics Laboratory
University of Washington
1013 NE 40th Street
Seattle, WA 98105-6698

8. PERFORMING ORGANIZATION REPORT NUMBER
APL-UW TM31-93

9. SPONSORING / MONITORING AGENCY NAME(S) AND ADDRESS(ES)
Naval Research Laboratory
Stennis Space Center, MS 39529-5004

10. SPONSORING / MONITORING AGENCY REPORT NUMBER

11. SUPPLEMENTARY NOTES

12a. DISTRIBUTION / AVAILABILITY STATEMENT
Approved for Public Release; Distribution is unlimited.

12b. DISTRIBUTION CODE

13. ABSTRACT *(Maximum 200 words)*

Initial research on a new method for characterizing the acoustic properties of a shallow water site is documented. The method uses moored vertical transmitting and receiving arrays. By combining the array data with limited environmental data, the measured acoustic data are extrapolated to predict the coherent field and transmission loss over an extended region. Motivation for the problem and approach is given, and the theory of the extrapolation algorithm is presented. Numerical examples demonstrate the relative insensitivity of the method to knowledge about the sediment. An experiment to test the extrapolation procedure is contemplated for the summer of 1994, and a possible site off the Massachusetts-New Hampshire coast is considered. Using archival sound speed data and bathymetry, transmission loss is calculated for a region with a gently sloping bottom and is compared with extrapolated predictions. The extrapolation method is shown to be relatively insensitive to sound speed variability in the water column, but sensitive to changes in depth. Element spacing of greater than one-half the acoustic wavelength in both the transmitting and receiving arrays is shown to be adequate for some cases.

14. SUBJECT TERMS
Ocean acoustics
Normal mode theory
Shallow water propagation
Acoustic calibration
Huygen's principle
Field extrapolation

15. NUMBER OF PAGES
34

16. PRICE CODE

17. SECURITY CLASSIFICATION OF REPORT	18. SECURITY CLASSIFICATION OF THIS PAGE	19. SECURITY CLASSIFICATION OF ABSTRACT	20. LIMITATION OF ABSTRACT
Unclassified	Unclassified	Unclassified	SAR